Can Scalar Fields Lead to an Accelerating Universe?

Edward Miller

14323612

Abstract

We review the origins of the Friedmann equations and the cosmological constant problem. We then consider a flat FRW model universe containing a scalar field with a potential $V = V_0 e^{-k\lambda\phi}$ *and a general barotropic fluid. A dark energy solution is found along with a tracking solution which is determined to be the preferential fixed point. The model is extended to a universe containing matter, radiation, and a scalar field simultaneously. Here, we find two tracking solutions corresponding to matter and radiation respectively, along with the original dark energy solution. The matter tracking solution is found to be the preferential fixed point. Finally, the potential is modified to include a second exponential. Here, we find two regimes. In the first, exists the previous fixed points along with counter parts in terms of a new parameter,* σ*. In the second, we find a new dark energy solution corresponding to a constant field. This is shown to be the preferential fixed point of the system, so we argue this sufficiently concludes that a scalar field with an exponential potential is a viable dark energy candidate. We also note the existence of temporary periods of acceleration during domination by the kinetic contribution of the field.*

Contents

1. Introduction. 3

1.1 Dark energy and the Friedmann equations. 3

1.2 The Cosmological Constant. 5

1.3 Scalar Fields. 7

2. Universe Containing a Baryotropic Fluid and a Scalar Field. 8

2.1 Evolution equations, Phase plane analysis and Critical points. 8

2.2 Acceleration Condition, Density Parameter and Effective Equation of State. 10

2.3 Stability Analysis. 10

2.4 Numerical Solutions. 12

2.5 Results and Discussion. 15

3. Universe Containing Matter, Radiation, and a Scalar Field. 17

3.1 Evolution Equations, Phase Plane Analysis and Critical points (3D). 17

3.2 Acceleration Condition, Density Parameter and Effective Equation of State (3D). . 18

3.3 Stability Analysis (3D). 19

3.4 Numerical Solutions (3D). 20

3.5 Results and Discussion (3D). 23

4. Modified Potential. 24

4.1 Results and Discussion (4D). 26

5. Conclusion. 28

1. Introduction

The expansion of the universe was famously observed by Edwin Hubble in 1929.[1] By comparing the change in redshift from distant nebulae, later discovered to be galaxies, it was found that distant objects were receding from us with a velocity proportional to distance. This became known as the Hubble-Lemaitre law, given by $v = Hr$, where v is the recession velocity, H is the Hubble parameter and r is distance. If we apply the cosmological principle, that the universe is homogenous and isotropic, then this implies an expanding universe. Later in 1998, more accurate measurements of type 1a supernovae confirmed that the expansion was accelerating. [2]

It was previously thought that the energy density of the universe today was dominated by matter and so the combined gravitational contribution from both dark and baryonic matter should cause decelerating expansion. However, this is contrary to what is observed. Instead, there must be some yet undetermined contribution to the energy density of the universe acting over cosmological scales against the matter contribution. This is known as dark energy and, as verified with increasing precision by recent observational evidence, makes a significant contribution to the total energy density of the universe. Although many models exist, dark energy is most commonly attributed to a constant vacuum energy appearing as a cosmological constant in the evolution equations governing the expansion.

1.1 Dark Energy and the Friedmann Equations

To describe the evolution of the universe we start with Einstein's field equations of general relativity. [3] These relate the geometry of a region of spacetime to the matter/energy distribution contained within and can be written in terms of mixed components as[1]

$$R_\nu^\mu - \frac{1}{2}\delta_\nu^\mu R = 8\pi G T_\nu^\mu \tag{1}$$

where R_ν^μ is the Ricci tensor which encodes the geometry of a region of spacetime, δ_ν^μ is the Kronecker delta, R is the Ricci scalar, G is the gravitational constant and T_ν^μ is the energy – momentum tensor which combines the matter/energy distribution into a single source term. [2] The Ricci scalar is the contraction of the Ricci tensor with the metric tensor, $R = g^{\mu\nu}R_{\mu\nu}$ where the metric tensor, $g^{\mu\nu}$, defines the geometry of a surface such that the line element, ds, between two points is given by $ds^2 = g_{\mu\nu}dx^\mu dx^\nu$. The spatial geometry of the universe has uniform curvature and corresponds to the Friedman-Robertson-Walker (FRW) metric in which ds is given by the following, [3]

$$ds^2 = dt^2 - a^2(t)\left[\frac{dr^2}{1-Kr^2} + r^2(d\theta^2 + sin^2\theta d\phi^2)\right], \tag{2}$$

where $a(t)$ is the scale factor relating the size of the universe at time t to its current size[3] and K is the curvature. Positive K corresponds to closed geometry such as that of a sphere and negative K to

[1] Standard index notation used such that Greek indices, $\mu, \nu \dots$, notate spacetime components and Latin, $i, j, k, \dots$, used to notate Euclidean components. 3-vectors denoted by bold print e.g., $\boldsymbol{V}$.

[2] Natural units ($c = \hbar = 1$) and Einstein summation convention (repeated indices summed over) used unless stated otherwise.

[3] $a_0 = 1$ defined as the scale factor today.

open geometry such as a hyperbolic surface. The temporal and spatial components of the Ricci tensor in this geometry are [4]

$$R_0^0 = \frac{3\ddot{a}}{a}, \tag{3}$$

$$R_j^i = (\frac{\ddot{a}}{a} + \frac{2\dot{a}^2}{a} + \frac{2K}{a})\delta_j^i \ , \tag{4}$$

respectively where dots denote derivatives with respect to time. The Ricci scalar is given by

$$R = 6\left(\frac{\ddot{a}}{a} + \frac{\dot{a}^2}{a^2} + \frac{K}{a^2}\right). \tag{5}$$

If we approximate all contributions to the energy density of the universe as a perfect fluid, then the energy-momentum tensor becomes a diagonal matrix of the form

$$T_\nu^\mu = diag(-\rho, p, p, p). \tag{6}$$

where the density and pressure of the fluid are given by ρ and p respectively. Now, considering just the temporal component of the Ricci tensor, we notice that due to the Kronecker delta and the diagonality of T_ν^μ, equation (1) will only be non-zero when $\mu = \nu = 0$ on both sides. Therefore, substituting $T_0^0 = -\rho$ into (1) along with R and R_0^0 and rearranging for $(\dot{a}/a)^2$ gives us

$$H^2 \equiv \left(\frac{\dot{a}}{a}\right)^2 = \frac{8\pi G}{3}\rho - \frac{K}{a^2} \tag{7}$$

where we have used the relation between distances now and distances at a time, t, $r(t) = a(t)r(t_0)$, to define the Hubble parameter, H. We can now consider any spatial component of R_ν^μ and use the fact that the only non-zero terms will be when $i = j$ on both sides. Using this property, along with (7), allows us to obtain the acceleration equation,

$$\frac{\ddot{a}}{a} = -\frac{4\pi G}{3}(\rho + 3p). \tag{8}$$

Equations (7) and (8) are the Friedmann equations and relate the expansion rate of the universe to its spatial curvature as well as the energy density and pressure of a cosmological fluid. The density, ρ, is an abbreviation of the total density and is given by $\rho = \sum_i \rho_i$ where i runs over all contributions e.g. matter, radiation etc. Finally, we derive the fluid equation by taking the time derivative of (7) and substituting $\ddot{a}/a$ with (8).

Rearranging and using the definition of H gives

$$\dot{\rho} + 3H(\rho + p) = 0. \tag{9}$$

We also define the dimensionless density parameter, Ω, as the ratio of the density to the critical density, ρ_c. The critical density is defined as the density required for a spatially flat universe $(K = 0)$ and so from (7), must take the form $\rho_c = 3H^2/8\pi G$.

The density parameter can therefore be written as

$$\Omega = \frac{\rho}{\rho_c} = \frac{8\pi G}{3H^2}\rho \tag{10}$$

with $\Omega = \sum_i \Omega_i$ where i runs over all contributions. This allows us to re-write the Friedmann equation, (7), in terms of the density parameter. By dividing by ρ_c and rearranging, (7) becomes

$$1 = \Omega - \frac{K}{H^2a^2}. \tag{11}$$

Now, if we define the curvature density parameter to be $\Omega_k = -K/H^2a^2$ we have the following,

$$1 = \Omega + \Omega_k \tag{12}$$

Observations of the cosmic microwave background (CMB) released in 2018 from the Planck satellite, [5] give the contribution from the curvature as $\Omega_k = 0.001 \pm 0.002$ which is consistent with a flat universe. Consequently, we arrive at the constraint, $\Omega = \sum_i \Omega_i = 1$. The Planck results give the matter contribution as $\Omega_m = 0.315 \pm 0.007$ and so, assuming all other contributions such as radiation are negligible, we see from our constraint that dark energy contributes approximately 70% of the energy density in the universe.

1.2 The Cosmological Constant

The idea of a cosmological constant was introduced by Einstein to satisfy his belief that the universe must be static, $\dot{a} = 0$. If we impose this constraint on (7) we are left with

$$\frac{K}{a^2} = \frac{8\pi G}{3}\rho \tag{13}$$

and from the acceleration equation, (8), we obtain $3p = -\rho$. Using this relation with (13) then tells us that for a static universe

$$\rho = -3p = \frac{3K}{8\pi G a^2}\,. \tag{14}$$

We see the denominator must be positive and so, for the expression to be non-zero, K must be positive or negative. This implies that either ρ or p must be negative but as negative energy density is unphysical, we must conclude that the cosmological fluid makes a negative contribution to the pressure. Intuitively, we begin to see the connection with dark energy as we require a negative pressure contribution to act against gravity on cosmic scales. Einstein, firm in his belief of a static universe, thought this result could not correspond to the real universe and so added an additional term, Λ, to the field equations.

With this added cosmological constant (1) becomes

$$R^{\mu}_{\nu} - \frac{1}{2}\delta^{\mu}_{\nu}R + \Lambda\delta^{\mu}_{\nu} = 8\pi G T^{\mu}_{\nu}\,. \tag{15}$$

Hence, following the same method used to derive (7) and (8), we arrive at the modified Friedmann equations

$$H^2 \equiv \left(\frac{\dot{a}}{a}\right)^2 = \frac{8\pi G}{3}\rho - \frac{K}{a^2} + \frac{\Lambda}{3}\,, \tag{16}$$

$$\frac{\ddot{a}}{a} = -\frac{4\pi G}{3}(\rho + 3p) + \frac{\Lambda}{3}\,. \tag{17}$$

Now, returning to Einstein's requirement that the universe be static, from (16) we have

$$\frac{K}{a^2} = \frac{8\pi G}{3}\rho + \frac{\Lambda}{3} \tag{18}$$

and from (17),

$$\frac{4\pi G}{3}(\rho + 3p) = \frac{\Lambda}{3}\,. \tag{19}$$

Defining the equation of state of a fluid to be[4]

$$w = (\gamma - 1) = \frac{P}{\rho} \tag{20}$$

and using the fact that for matter $w \approx 0$ [6] we conclude that $p_m \approx 0$. Hence, substituting into (18) and (19) and combining the two gives us

$$\rho \propto \Lambda = \frac{K}{a^2} \tag{21}$$

from which it is clear that Λ must be positive. This implies that Einstein's static universe must be closed as K must also be positive. From [5] we see that this is not the case and even at the time of publishing astronomers such as Slipher [7] were beginning to measure the spectral lines of galaxies and so there was growing evidence that the universe was not static as Einstein postulated.

The cosmological constant was discarded with the acceptance of an expanding universe. However, with the publishing of better distance measurements in the 1990s, it was noticed that the presence of such a constant contributing a negative pressure could explain the observed accelerating expansion. The constant's origin can be attributed to a zero-point energy of the vacuum. However, calculations of its value using Quantum Field Theory result in a discrepancy between the calculated value and the value required to produce the observed acceleration today. This is known as the Cosmological constant problem.

Astronomical observations give an upper bound of $|\Lambda| < 10^{-56} cm^{-2}$ [8] which can be converted into a bound on the vacuum energy density, $|\rho_{vac}| \lesssim 10^{-16} J cm^{-3}$. To compare this with the energy density of the vacuum, we can consider just the contribution from the electromagnetic field as a group of Quantum Harmonic Oscillators (QHO)s to approximate a lower bound on ρ_{vac}. The QHO has a zero-point energy $E_0 = (1/2)\hbar\omega$ where $\hbar$ is the reduced Planck's constant and ω is the frequency[5]. This can be demonstrated by solving the Schrödinger equation in the systems ground state. We can define a quantum Hamiltonian for the electromagnetic field by promoting the components, **E**(**x**,t) and **B**(**x**,t), to operators in the classical Hamiltonian,

$$H = \frac{E^2 + B^2}{2}. \tag{22}$$

In Quantum Electro Dynamics (QED) the zero-point energy is given by [8]

$$E_0 = \langle 0|\hat{\mathrm{H}}|0\rangle = \frac{1}{2}\langle 0| \int \left(\hat{E}^2 + \hat{B}^2\right) d^3x |0\rangle = \delta^3(0)\frac{1}{2}\int \hbar\omega_k d^3k \tag{23}$$

where we have integrated over a continuum of modes of the electromagnetic field with wavevector k. $\delta^3(0)$ is the 3d delta function and $|0\rangle$ is the vacuum state. Equation (23) results in an infinite energy but, assuming our theory is valid only up to a certain scale, we can define a cut off frequency, ω_{max}. $\delta^3(0)$ can be made finite via regularization in which quantities are modified by introducing an extra parameter known as the regulator.[8] By introducing a box of volume, V, we can use the equivalence of a mode of the field with that of the quantum harmonic oscillator. Therefore, we find the energy per unit volume by summing over all frequencies up to ω_{max}.

$$\rho_{vac} = \frac{E}{V} = \frac{1}{V}\sum\nolimits_k \frac{1}{2}\hbar\omega_k \,. \tag{24}$$

[4] γ and w used interchangeably as the equation of state of a fluid. Later, γ is used instead of w.
[5] Factors of $\hbar$ and c restored temporarily.

In the limit $V \to \infty$ this becomes the integral,

$$\rho_{vac} = \frac{\hbar}{2\pi^2 c^3} \int_0^{\omega_{max}} \omega^3 \, d\omega \ , \tag{25}$$

which, when evaluated, gives

$$\rho_{vac} = \frac{\hbar}{8\pi^2 c^3} {\omega_{max}}^4 \ . \tag{26}$$

Taking ω_{max} to be the frequency associated with the Planck energy, $E_{Pl} \sim 10^{19} GeV$, and using (26) we arrive at an energy density $\rho_{vac} \sim 10^{106} Jcm^{-3}$. This is over a hundred orders of magnitude greater than observed. Efforts can be made to produce energies matching the observed value however, these require techniques such as renormalization [9] which were heavily criticized by one of the pioneers of QED, Richard Feynman, and remain controversial in the physics community. Either way, a discrepancy of this scale highlights issues with the theory.

1.3 Scalar Fields

With the vacuum energy proving to be an inadequate source of dark energy, we must look towards alternative explanations to find the cause of today's accelerating expansion. A different approach, and the focus of this investigation, will be to consider the existence of a scalar field. They are defined to be invariant under Lorentz transformations and, in Quantum Field Theory, correspond to relativistic spin-zero bosons. [10]

Scalar field models have been shown to be suitable candidates to drive the process of inflation [3], a period of exponential expansion in the early universe. Scalar fields have been observed experimentally via the Higgs boson [11] and so it is only natural to consider such a field as a possible source of dark energy. In our investigation we will consider a similar scalar field, ϕ, with potential, $V(\phi)$, and an associated energy-momentum tensor given by [3]

$$T_{\mu\nu} = (\partial_u \phi)(\partial_\nu \phi) - g_{\mu\nu}[\tfrac{1}{2}(\partial_\sigma \phi)(\partial^\sigma \phi) - V(\phi)] \ . \tag{27}$$

where, ∂_μ, are shorthand for $\partial/\partial x_\mu$ with x_μ being a component of a general spacetime coordinate. If we assume ϕ acts as a perfect fluid, we can compare (27) with (3) and hence derive expressions for the density and pressure of our scalar field. To do this, we re-write the components of (3) as

$$T_{\mu\nu} = (\rho + p) u_\mu u_\nu - p g_{\mu\nu} \tag{28}$$

where $u_\mu$are the components of a general 4-vector. It can be shown this is equal to (3) if we take the approximation that, in the rest frame of the fluid, curvature of spacetime due to mass is negligible. This means $g_{\mu\nu} = \eta_{\mu\nu}$ where $\eta_{\mu\nu}$ is the Minkowski metric defining the geometry of flat space time and is given by $\eta_{\mu\nu} = diag(-1,1,1,1)$. Then, using relations, $u_\mu = \eta_{\mu\nu} u^\nu$ and $u^\nu u_\nu = 1$ (in natural units) we see that (3) and (28) are indeed equivalent. Finally, by comparing the forms of (27) and (28) we find the density, ρ_ϕ, and the pressure, p_ϕ, of the scalar field given by

$$\rho_\phi = \tfrac{1}{2}\dot{\phi}^2 + V(\phi) + \tfrac{1}{2}(\boldsymbol{\nabla}\phi)^2 \ , \tag{29}$$

$$p_\phi = \tfrac{1}{2}\dot{\phi}^2 - V(\phi) - \tfrac{1}{6}(\boldsymbol{\nabla}\phi)^2 \ . \tag{30}$$

It can be seen, using (20), that if ϕ is constant then it will have an equation of state, $w = -1$, as required by a dark energy candidate. Our investigation will consider a similar form that varies in time only.

2. Universe Containing a Baryotropic Fluid and a Scalar Field

We first consider a model universe containing our scalar field, ϕ, and a general fluid with a baryotropic equation of state, γ where $0 \leq \gamma \leq 2$, such that the pressure and density of the fluid are related by [12] $p_\gamma = (\gamma - 1)\rho_\gamma$. We will consider a scalar field with density and pressure of the form (29) and (30). Assuming it is spatially constant, these are given by

$$\rho_\phi = \frac{1}{2}\dot{\phi}^2 + V(\phi)\,, \tag{31}$$

$$p_\phi = \frac{1}{2}\dot{\phi}^2 - V(\phi)\,. \tag{32}$$

The primary goal of the investigation will be to see whether such a field, with an exponential potential of the form,

$$V = V_0 e^{-k\lambda\phi}\,, \tag{33}$$

is sufficient to cause accelerating expansion. λ is a parameter giving the growth rate of the exponential and V_0 is a constant.

2.1 Evolution Equations, Phase Plane Analysis and Critical Points

To find the evolution equations we begin with a spatially flat universe in the FRW geometry and take $\Lambda = 0$. Taking the total energy density of the universe to be $\rho = \rho_\phi + \rho_\gamma$ and using (7) we therefore have,

$$H^2 = \frac{k^2}{3}\left[\rho_\gamma + \frac{1}{2}\dot{\phi}^2 + V(\phi)\right], \tag{34}$$

where we let $k = 8\pi G$. The next two evolution equations are trivial as each fluid has an associated fluid equation,

$$\dot{\rho}_\gamma + 3H\left(\rho_\gamma + p_\gamma\right) = 0\,, \tag{35}$$

$$\dot{\rho}_\phi + 3H\left(\rho_\phi + p_\phi\right) = 0\,. \tag{36}$$

To find the time evolution of the scalar field we substitute our expressions for the density and pressure, (31) and (32), into the fluid equation, (36), yielding

$$\ddot{\phi} + 3H\dot{\phi} + \frac{dV}{d\phi} = 0\,. \tag{37}$$

We obtain our final evolution equation by differentiating (7) with respect to time giving,

$$2H\dot{H} = \frac{k^2}{3}\left(\dot{\rho}_\phi + \dot{\rho}_\gamma\right). \tag{38}$$

After substituting with (34), (35) and using expressions (31) and (32) we finally arrive at,

$$\dot{H} = -\frac{k^2}{2}\left(\rho_\gamma + p_\gamma + \dot{\phi}^2\right), \tag{39}$$

giving us a universe with evolution described by (34), (35), (36), (37), and (39). To find the fixed points of this system we must reduce our evolution equations to a 2D, autonomous system. This is achieved by introducing the dimensionless parameters

$$x = \frac{k\dot{\phi}}{\sqrt{6}H}\,, \qquad y = \frac{k\sqrt{V}}{\sqrt{3}H}\,, \qquad N = \ln\left(a\right). \tag{40}$$

Firstly, we write the Friedman equation, (34), as the constraint,

$$\frac{\rho_\gamma k^2}{3H^2} = 1 - x^2 - y^2 \ . \tag{41}$$

Rearranging x gives $H = k\dot{\phi}/\sqrt{6}x$ and taking derivatives with respect to time obtains,

$$\dot{H} = \frac{k\ddot{\phi}}{\sqrt{6}x} - \frac{k\dot{\phi}}{\sqrt{6}x^2}\frac{dx}{dt} \ . \tag{42}$$

We now notice that, using the chain rule, dx/dt can be written as,

$$\frac{dx}{dt} = \frac{dx}{dln(a)}\frac{dln(a)}{dt} = x'H \tag{43}$$

where we have defined $x' = dx/dN$. Using this definition in (42) and equating with (39) gives

$$-\frac{k^2}{2}\left(\rho_\gamma + p_\gamma + \dot{\phi}^2\right) = \frac{k\ddot{\phi}}{\sqrt{6}x} - \frac{k\dot{\phi}}{\sqrt{6}x^2}x'H \ . \tag{44}$$

We can replace $\ddot{\phi}$ with equation (37) and write P_γ in terms of ρ_γ using the equation of state. If we make use of the fact that $dV/d\phi = -\lambda kV$ and substitute for the definitions of x, y along with the constraint (41), we obtain the first equation in x and y,

$$x' = -3x + \lambda\sqrt{\frac{3}{2}}y^2 + \frac{3}{2}x[2x^2 + \gamma(1 - x^2 - y^2)] \ . \tag{45}$$

Performing a similar calculation beginning with y gives us the second,

$$y' = -\lambda\sqrt{\frac{3}{2}}xy + \frac{3}{2}y[2x^2 + \gamma(1 - x^2 - y^2)] \tag{46}$$

with $y' = dy/dN$ and so the evolution equations of our model have been reduced to the 2D autonomous system specified by (45) and (46).

To find the fixed points we take $x' = y' = 0$ and rearrange to find x and y in terms of parameters λ and γ. The first three fixed points, which we shall refer to as (A), (B) and (C), are identified as

$$\text{(A): } x = y = 0 \ , \qquad \text{(B): } x = 1 \ , \ y = 0 \ , \qquad \text{(C): } x = -1 \ , y = 0 \ , \tag{47}$$

and exist for all values of λ. The fourth point, (D), is found to be

$$\text{(D): } x = \frac{\lambda}{\sqrt{6}} , y = \sqrt{1 - \frac{\lambda^2}{6}} , \tag{48}$$

and as x and y must be real valued to make physical sense, we see that (D) only exists for $\lambda^2 < 6$. The final point, (E), is given by

$$\text{(E): } x = \sqrt{\frac{3}{2}}\frac{\gamma}{\lambda} , y = \sqrt{\frac{3(2-\gamma)\gamma}{2\lambda^2}} . \tag{49}$$

The Friedmann constraint, (41), implies the condition $x, y < 1$ and so we see that point (E) can only exist for $\lambda^2 > 3\gamma$.

2.2 Acceleration Condition, Density Parameter and Effective Equation of State

To assess if our scalar field is a dark energy candidate, we must define the condition on x and y required for accelerating expansion. Acceleration is defined as

$$\ddot{a} > 0 \,. \tag{50}$$

Using the definition of the Hubble parameter, $H = \dot{a}/a$, we can re-write this inequality as

$$a\left(\dot{H} + H^2\right) > 0 \tag{51}$$

however, by definition $a > 0$ which implies

$$\dot{H} + H^2 > 0 \,. \tag{52}$$

If we replace $\dot{H}$ using (39) and use the definition of the equation of state to remove p_γ, we arrive at

$$-\frac{k^2}{2}\left(\gamma\rho_\gamma + \dot{\phi}^2\right) + H^2 > 0 \,. \tag{53}$$

By replacing ρ_γ using the constraint (41) and making the appropriate substitution for x, we hence obtain the acceleration condition in x and y,

$$\frac{1-3x^2}{1-x^2-y^2} > \frac{3}{2}\gamma \,. \tag{54}$$

The density parameter, Ω , is defined by (10) and so using the expression for the energy density of the field, (31), and after substituting for x and y we have

$$\Omega_\phi = x^2 + y^2 \,. \tag{55}$$

The final parameter we wish to define is the effective equation of state of the scalar field, γ_ϕ. We know from (20) $p_\phi = (\gamma_\phi - 1)\rho_\phi$ and so

$$\gamma_\phi = \frac{p_\phi + \rho_\phi}{\rho_\phi}, \tag{56}$$

which, when using expressions (31) and (32), becomes

$$\gamma_\phi = \frac{\dot{\phi}^2}{\frac{1}{2}\dot{\phi}^2 + V} \,. \tag{57}$$

Finally, expressing in terms of x and y gives us

$$\gamma_\phi = \frac{2x^2}{x^2+y^2} \,. \tag{58}$$

2.3 Stability Analysis

To analyze the stability of our 2D system we consider perturbations, $u_1$and u_2, around the general fixed point (x^*, y^*) such that,

$$u_1 = x - x^*, \tag{59}$$

$$u_2 = y - y^* \,. \tag{60}$$

Our system, given by (45) and (46), can be written more generally as

$$x' = f_1(x, y)\ , \tag{61}$$

$$y' = f_2(x, y)\ . \tag{62}$$

If we consider just (61) and take the Taylor expansion around the fixed point, we can use the fact that $x' = {u_1}'$ to write,

$${u_1}' = f_1(x^*, y^*) + u_1 \frac{\partial f_1}{\partial x}_{x=x^*, y=y^*} + u_2 \frac{\partial f_1}{\partial y}_{x=x^*, y=y^*} + \cdots \quad . \tag{63}$$

As long as the perturbations are small, we can ignore terms higher than first order. By definition $f(x^*, y^*) = 0$ and so expanding (61) and (62) in this way allows us to express our 2D system in vector form,

$$\begin{bmatrix} {u_1}' \\ {u_2}' \end{bmatrix} = \begin{bmatrix} \frac{\partial f_1}{\partial x} & \frac{\partial f_1}{\partial y} \\ \frac{\partial f_2}{\partial x} & \frac{\partial f_2}{\partial y} \end{bmatrix}_{\mathbf{x}=\boldsymbol{x}^*} \begin{bmatrix} u_1 \\ u_2 \end{bmatrix}, \tag{64}$$

which can be written more compactly as $\boldsymbol{u}' = J\boldsymbol{u}$ **.** This has a general solution,

$$\begin{bmatrix} u_1 \\ u_2 \end{bmatrix} = \begin{bmatrix} A_1 & A_2 \\ B_1 & B_2 \end{bmatrix} \begin{bmatrix} e^{m_1 N} \\ e^{m_2 N} \end{bmatrix}\ , \tag{65}$$

where A_1, A_2, B_1, B_2 are constants and $m_1$and m_2 are the eigenvalues of matrix J. It is clear then, that the stability of the fixed point depends on $m_1$and m_2 as the point will be stable if the real parts of $m_1$and m_2 are negative.

The stability of the fixed points (A) to (E) can therefore be found by evaluating J at each point and calculating its eigenvalues. The fixed points and their associated eigenvalues are given in table 1.

Table 1: Fixed points and associated eigenvalues

Point:	x	y	Eigenvalues:
(A):	0	0	$m_1 = \frac{3}{2}\gamma,\ m_2 = \frac{3}{2}(\gamma - 2)$
(B):	1	0	$m_1 = 3(2-\gamma),\ m_2 = \sqrt{\frac{3}{2}}(\sqrt{6} - \lambda)$
(C):	-1	0	$m_1 = 3(2-\gamma),\ m_2 = \sqrt{\frac{3}{2}}(\sqrt{6} + \lambda)$
(D):	$\frac{\lambda}{\sqrt{6}}$	$\sqrt{1 - \frac{\lambda^2}{6}}$	$m_1 = \lambda^2 - 3\gamma,\ m_2 = \frac{1}{2}(\lambda^2 - 6)$
(E):	$\sqrt{\frac{3}{2}}\frac{\gamma}{\lambda}$	$\sqrt{\frac{3(2-\gamma)\gamma}{2\lambda^2}}$	$m_{1,2} = -\frac{3}{4}(2-\gamma)\left[1 \pm \sqrt{1 - \frac{8\gamma}{\lambda^2}\left(\frac{\lambda^2 - 3\gamma}{2-\gamma}\right)}\right]$

From analysis of the eigenvalues, we find that point (A) is a saddle point for $0 < \gamma < 2$. As this is the range for which we have defined γ to exist, we conclude that (A) is always half stable. Point (B) we find to be stable for $\lambda > \sqrt{6}, \gamma > 2$, half stable for $\lambda < \sqrt{6}, \gamma > 2$ and unstable for $\lambda < \sqrt{6}$. (C) is stable for $\lambda < -\sqrt{6}, \gamma > 2$, half stable for $\lambda > \sqrt{6}, \gamma < 2$ and unstable for $\lambda > \sqrt{6}, \gamma < 2$. We again observe that points (B) and (C) are only stable for $\gamma > 2$ and so deduce that these points are never stable. (D) is stable for $\lambda^2 < 3\gamma$ and half stable in the range $3\gamma < \lambda^2 < 6$. (E) is found to be stable in the range $3\gamma < \lambda^2 < 24\gamma^2/(9\gamma - 2)$ and a stable spiral for $\lambda^2 > 24\gamma^2/(9\gamma - 2)$.

2.4 Numerical Solutions

For a graphical approach we solve our 2D system, given by (45) and (46), numerically using the Ode45 function in MATLAB. Ode45 solves first order, ordinary differential equations (ODEs) of the form,[6]

$$\frac{dx}{dt} = f(t, x)\,, \qquad x_0 = x(t_0)\,, \tag{66}$$

where x and t are the dependent and independent variables respectively. x_0 is the initial condition. To solve multiple, coupled, ODEs simultaneously we write (66) in MATLAB as a vector equation. dx/dt becomes a vector with (45) and (46) as components, t becomes a vector containing the range of values we wish to evaluate x at and x itself becomes a matrix with dimensions of length t by length x_0 containing the dependent variables evaluated at each value of t. x_0 becomes a vector of our chosen initial conditions. Solving numerically for different values of λ allows us to plot figures 1 to 6 with multiple trajectories plotted by running the code for a range of initial conditions.

[6] x is a general variable and not the parameter defined by (40).

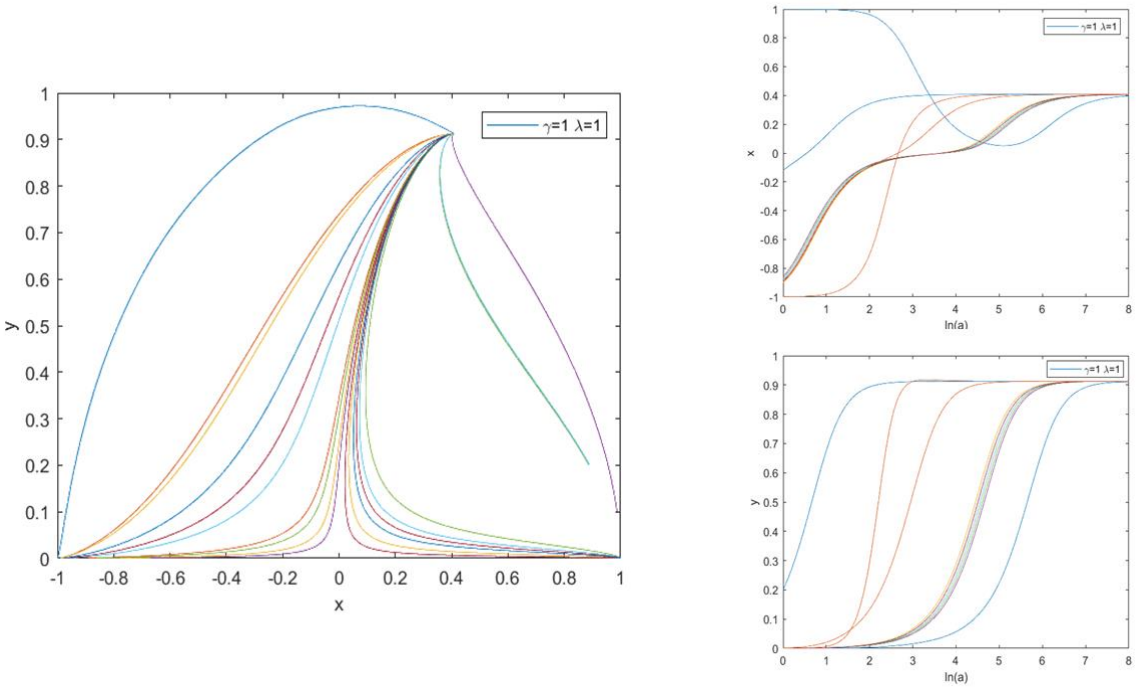

Figure 1: Phase plane of system for $\lambda = 1, \gamma = 1$. Plot of x against y (pictured left) shows trajectories converge at the fixed point $x = \sqrt{\frac{1}{6}}, y = \sqrt{\frac{5}{6}}$ in late times which corresponds to point (D). Individual plots of x against $\ln(a)$ (pictured top right) and y against $\ln(a)$ (pictured bottom right).

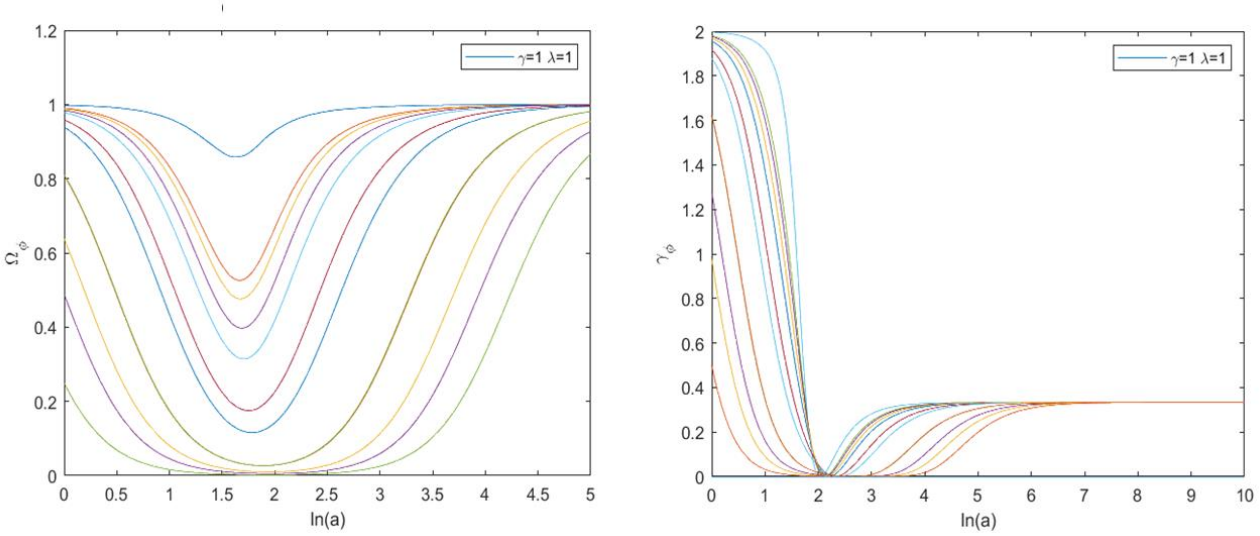

Figure 2: Plot of the density parameter, Ω_ϕ, against $\ln(a)$ for $\lambda = 1, \gamma = 1$ (pictured left). In late times Ω_ϕ goes to 1 and so scalar field dominates. Plot of effective equation of state, γ_ϕ, against $\ln(a)$ (pictured right). γ_ϕ goes to $1/3$. Plots confirm trajectories converge at point (D).

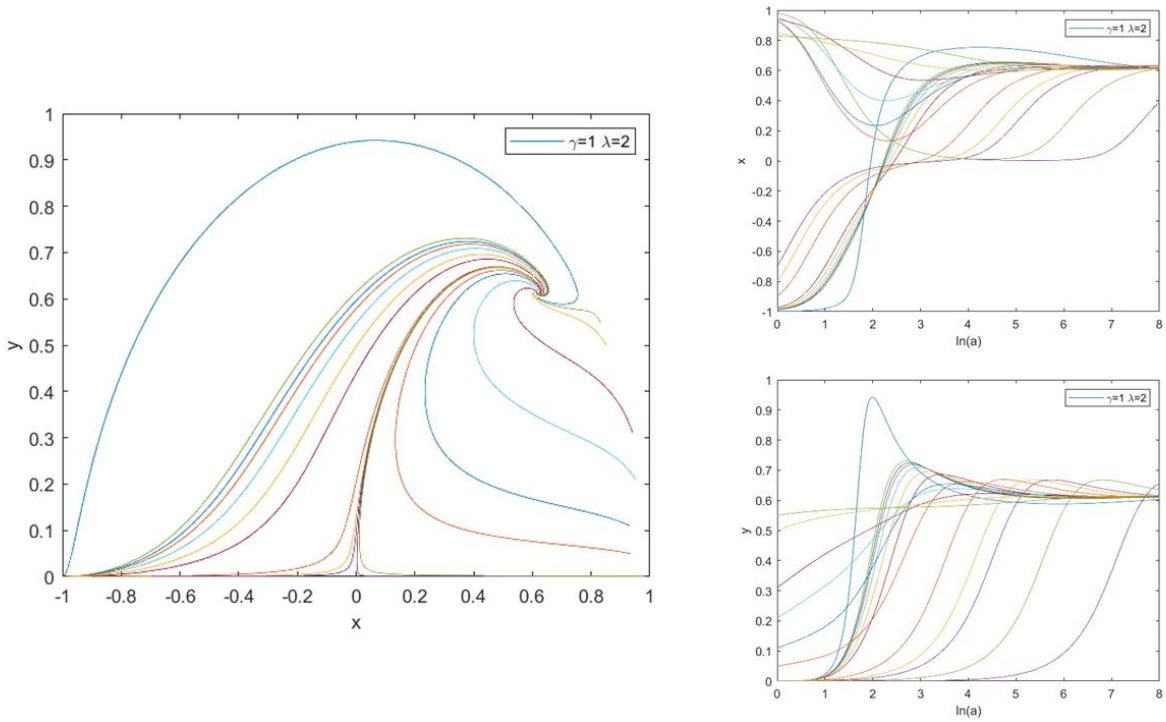

Figure 3: Phase plane for $\lambda = 2$ and $\gamma = 1$ (pictured left). Trajectories converge to fixed point at $x = y = \sqrt{\frac{3}{8}}$ in late times corresponding to point (E). Individual plots of x against $\ln(a)$ (pictured top right) and y against $\ln(a)$ (pictured bottom right).

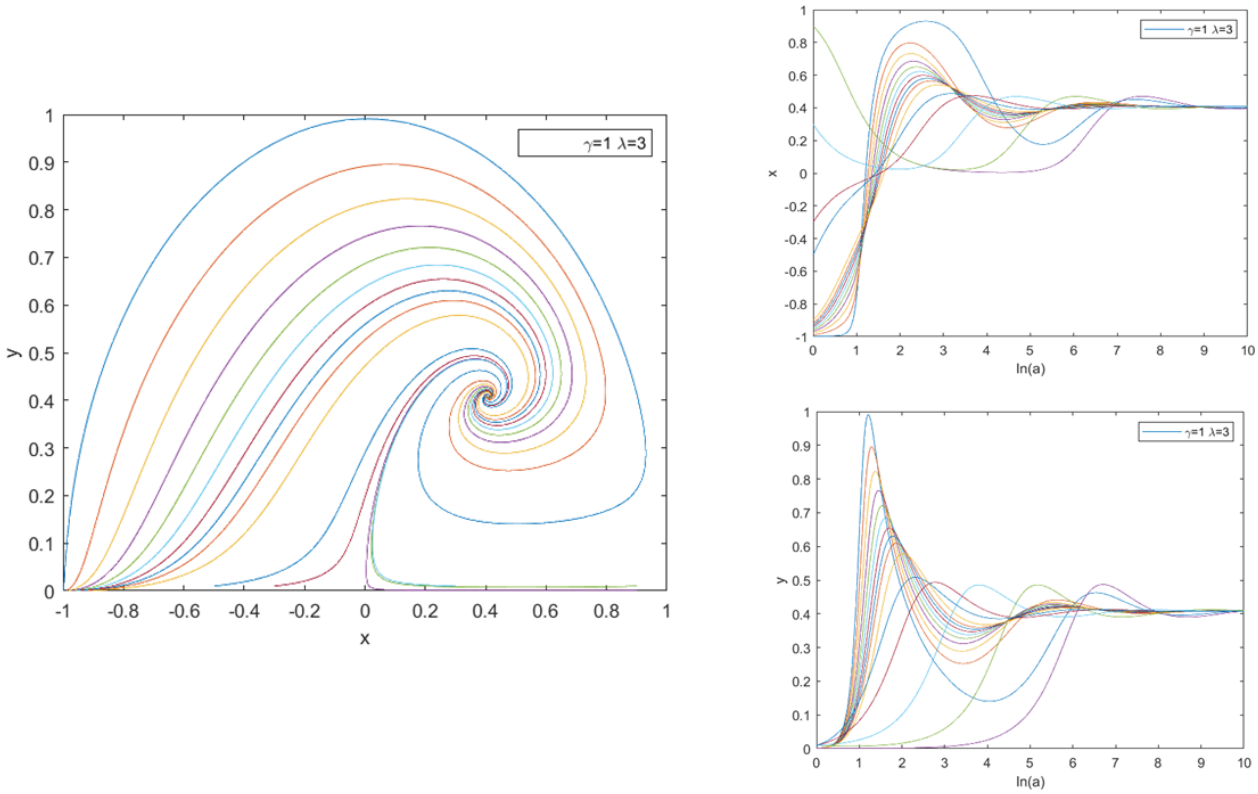

Figure 4: Phase plane for $\lambda = 3$ and $\gamma = 1$ (pictured left). Trajectories converge to fixed point at $x = y = \sqrt{\frac{1}{6}}$ in late times corresponding to point (E). Individual plots of x against $\ln(a)$ (pictured top right) and y against $\ln(a)$ (pictured bottom right.

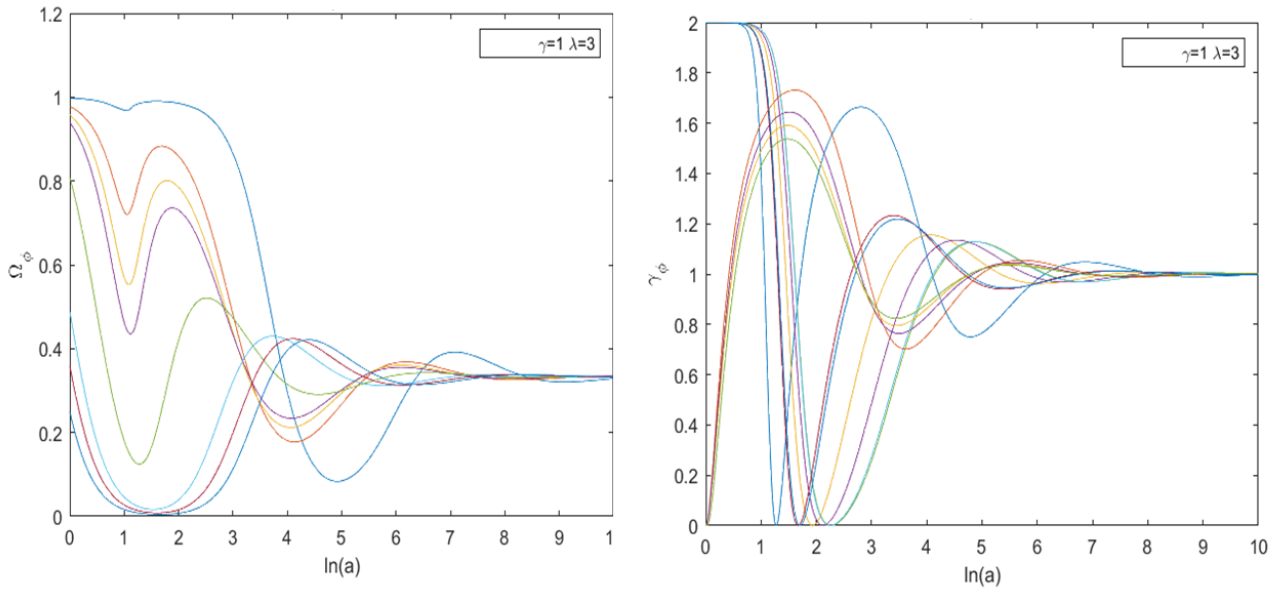

Figure 5: Plot of Ω_ϕ against $\ln(a)$ for $\lambda = 3$ and $\gamma = 1$ (pictured left). Ω_ϕ goes to $\frac{1}{3}$ in late times. Plot of effective equation of state, γ_ϕ, against $\ln(a)$ for $\lambda = 3$ and $\gamma = 1$ (pictured right). γ_ϕ goes to 1 in late times.

2.5 Results and Discussion

Having calculated all the necessary quantities derived in previous sections, the fixed points and all their properties are summarized in table 2.

Table 2: Fixed points and their associated properties

Point:	x	y	Existence criteria:	Stability:	Ω_ϕ	γ_ϕ	Acceleration condition satisfied?
(A)	0	0	$All\ \lambda\ and\ \gamma$	$Saddle\ point\ for\ 0 < \gamma < 2$	0	$undefined$	no
(B)	1	0	$All\ \lambda\ and\ \gamma$	$Unstable\ node\ for\ \lambda < \sqrt{6}$ $Saddle\ point\ for\ \lambda > \sqrt{6}$	1	2	no
(C)	-1	0	$All\ \lambda\ and\ \gamma$	$Unstable\ for\ \lambda > \sqrt{6}$ $Saddle\ point\ for\ \lambda < -\sqrt{6}$	1	2	no
(D)	$\frac{\lambda}{\sqrt{6}}$	$(1-\frac{\lambda^2}{6})^{\frac{1}{2}}$	$\lambda^2 < 6$	$Stable\ for\ \lambda^2 < 3\gamma$ $Saddle\ point\ for\ 3\gamma < \lambda^2 < 6$	1	$\frac{\lambda^2}{3}$	$For\ \lambda^2 < 2$
(E)	$\sqrt{\frac{3}{2}}\frac{\gamma}{\lambda}$	$\left[\frac{3(2-\gamma)\gamma}{2\lambda^2}\right]^{\frac{1}{2}}$	$\lambda^2 > 3\gamma$	$Stable\ for\ 3\gamma < \lambda^2 < \frac{24\gamma^2}{9\gamma-2}$ $Stable\ spiral\ for\ \lambda^2 > \frac{24\gamma^2}{9\gamma-2}$	$\frac{3\gamma}{\lambda^2}$	γ	no

Immediately, we see from the final column that (D) satisfies the acceleration condition and so could conclude that a scalar field with potential, (33), is a viable dark energy candidate. This conclusion however, would be premature as further analysis shows things are not so straight forward.

Although we have stated that point (A) does not correspond to an accelerating universe, applying the acceleration condition gives us an important result. Requiring that (A) obeys the acceleration condition results in the inequality, $\gamma < \frac{2}{3}$. Since this does not depend on λ, it must be a condition on the equation of state of a general fluid. Thus, we derive the general result that a cosmological fluid with equation of state $\gamma > \frac{2}{3}$ will not cause accelerating expansion. If we take this to correspond to matter, $\gamma = 1$, or radiation, $\gamma = 4/3$, then we see that this condition is not fulfilled. At points (B) and (C) the scalar field dominates. However, they do not satisfy the acceleration and we can recall from section 2.3 that they are only stable for $\gamma > 2$. Therefore, they can never be stable and so can be ignored. Point (D) satisfies the acceleration condition and, as we see from the density parameter, the scalar field dominates at this point. There also exists a range of λ within the existence criteria for which the point is stable and can allow acceleration. We therefore conclude that this is a dark energy solution. The final point, (E), does not correspond to acceleration but still has interesting properties. From table 2 we see the field has an effective equation of state equal to that of the general fluid and so, can identify this point as a tracking solution where the field mimics the contribution from the background.

Despite (D) being a clear dark energy solution, further analysis of the stability combined with the numerical solutions show that this is not the preferential fixed point of the system. This is because the range in which (D) is half stable coincides with both stability conditions on (E). We also notice that (E) can only be stable, as implied by the existence condition, and so it can be argued that this is the preferable fixed point in late times. This is demonstrated graphically in figure 6 which shows the system moving from points (D) to (E) for initial conditions close to the boundary. It is clear then, in this model universe, a scalar field with a potential of (33) is not a likely dark energy candidate.

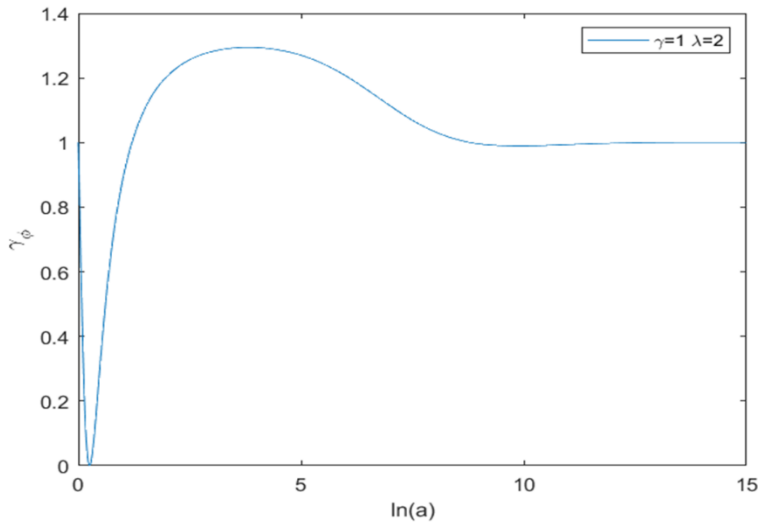

Figure 6: Plot of γ_ϕ against $\ln(a)$ for $\gamma = 1, \lambda = 3$. Choosing initial conditions $x = y = 0.7$, which lie close to the dark energy solution gives a trajectory of γ_ϕ that appears to move towards the dark energy solution $(\gamma_\phi = 1.33)$ before moving towards the stable tracking solution.

3. Universe Containing Matter, Radiation and a Scalar Field

We now consider a model universe like our own in which we replace the general baryotropic fluid with matter and radiation. Matter acts as a fluid with equation of state $\gamma_m = 1$ and radiation as one with $\gamma_r = 4/3$. They therefore contribute pressure $p_m = 0$ and $p_r = (1/3)\rho_r$ respectively where we will define ρ_r to be the energy density of radiation and ρ_m the density of matter. We will consider the same scalar field as the previous section.

3.1 Evolution Equations, Phase Plane Analysis and Critical points (3D)

To find the new evolution equations we make the following replacement in the Friedmann equation (34),

$$\rho_\gamma \to \rho_m + \rho_r \,, \tag{66}$$

giving,

$$H^2 = \frac{k^2}{3}\left[\rho_m + \rho_r + \frac{1}{2}\dot{\phi}^2 + V(\phi)\right]. \tag{67}$$

Since matter and radiation have their own fluid equations,

$$\dot{\rho}_m + 3H(\rho_m + p_m) = 0 \,, \tag{68}$$

$$\dot{\rho}_r + 3H(\rho_r + p_r) = 0 \,, \tag{69}$$

differentiating (67) and using (36), (68) and (69) to make the appropriate substitutions gives

$$\dot{H} = -\frac{k^2}{2}(\rho_m + \frac{4}{3}\rho_r + \dot{\phi}^2) \,. \tag{70}$$

As (36) and (37) remain unchanged, the evolution of the system is given by (36), (37), (67), (68), (69) and (70).

To conduct the phase plane analysis, we reduce these to a 3D autonomous system by introducing a new variable, z. We do this by considering the form of the constraint on the 2D system, (41). With the aim of making further calculations as simple as possible, we define z such that (67) can be written in a similar way as

$$\frac{\rho_m k^2}{3H^2} = 1 - x^2 - y^2 - z^2 \ . \tag{71}$$

By comparing with (67), we deduce that z takes the form,

$$z = \frac{k\sqrt{\rho_r}}{\sqrt{3}H} \,. \tag{72}$$

Using an identical method to that of section 2.1, the evolution of the system, given by (36), (37), (67), (68), (69) and (70), can be reduced to the 3D autonomous system,

$$x' = -3x + \lambda\sqrt{\frac{3}{2}}y^2 + x\left[2z^2 + 3x^2 + \frac{3}{2}(1 - x^2 - y^2 - z^2)\right], \tag{73}$$

$$y' = -\lambda\sqrt{\frac{3}{2}}xy + y\left[2z^2 + 3x^2 + \frac{3}{2}(1 - x^2 - y^2 - z^2)\right], \tag{74}$$

$$z' = -2z + 2z^3 + z\left[3x^2 + \frac{3}{2}(1 - x^2 - y^2 - z^2)\right], \tag{75}$$

where $z' = dz/dN$.

The fixed points are found by setting $x' = y' = z' = 0$ and are given, along with their existence criteria, in table 3.

Table 3: Fixed points of 3D system along with existence criteria

Point:	x	y	z	Existence criteria:
(A):	0	0	0	$All\ \lambda\ and\ \gamma$
(B):	1	0	0	$All\ \lambda\ and\ \gamma$
(C):	-1	0	0	$All\ \lambda\ and\ \gamma$
(D):	$\frac{\lambda}{\sqrt{6}}$	$(1-\frac{\lambda^2}{6})^{\frac{1}{2}}$	0	$\lambda^2 < 6$
(E):	$\frac{1}{\lambda}\sqrt{\frac{3}{2}}$	$\frac{1}{\lambda}\sqrt{\frac{3}{2}}$	0	$\lambda^2 > 3$
(F):	0	0	1	$All\ \lambda\ and\ \gamma$
(G)	$\frac{2}{\lambda}\sqrt{\frac{2}{3}}$	$\frac{1}{\lambda}\sqrt{\frac{4}{3}}$	$\sqrt{1-\frac{4}{\lambda^2}}$	$\lambda^2 > 4$

There is another fixed point at $x = y = 0$ and $z = -1$. However, as (73), (74) and (75) go as z^2 when $z \neq 0$ the point can be ignored.

3.2 Acceleration Condition, Density Parameter and Effective Equation of State (3D)

The density parameter and effective equation of state remain unchanged as they only depend on $\dot{\phi}$ and V and hence are still given by (55) and (58) respectively. The acceleration condition is easily adjusted for the new system. Starting with (52) we replace $\dot{H}$ using (70) and ρ_m using (71). After making further replacements for x and z we obtain

$$3y^2 - 3x^2 - z^2 > 1\ . \tag{76}$$

3.3 Stability Analysis (3D)

For the stability analysis, we use the same method as used in section 2.3. To generalize to a 3D system we define another perturbation, $u_3 = z - z^*$, and so the Taylor expansion of $x' = f_1(x, y, z)$ is

$$u_1{}' = f_1(x^*, y^*, z^*) + u_1 \frac{\partial f_1}{\partial x}_{x=x^*, y=y^*, z=z^*} + u_2 \frac{\partial f_1}{\partial y}_{x=x^*, y=y^*, z=z^*} + u_3 \frac{\partial f_1}{\partial z}_{x=x^*, y=y^*, z=z^*} \ldots . \quad (77)$$

Repeating for the $y'$and z' equations and ignoring terms higher than first order allows us to write our 3D system, (73), (74), (75), as a vector equation of the form $\boldsymbol{u}' = J\boldsymbol{u}$ where J is now the 3 by 3 matrix

$$J = \begin{bmatrix} \frac{\partial f_1}{\partial x} & \frac{\partial f_1}{\partial y} & \frac{\partial f_1}{\partial z} \\ \frac{\partial f_2}{\partial x} & \frac{\partial f_2}{\partial y} & \frac{\partial f_2}{\partial z} \\ \frac{\partial f_3}{\partial x} & \frac{\partial f_3}{\partial y} & \frac{\partial f_3}{\partial z} \end{bmatrix}. \quad (78)$$

We can, once again, find the stability by calculating the eigenvalues of J at each fixed point. The points and their eigenvalues are summarized in table 4.

Table 4: Fixed points of 3D system with associated eigenvalues

Point:	x	y	z	Eigenvalues:
(A):	0	0	0	$m_1 = -\frac{3}{2},\ m_2 = \frac{3}{2},\ m_3 = -\frac{1}{2}$
(B):	1	0	0	$m_1 = 3,\ m_2 = -\lambda\sqrt{\frac{3}{2}} + 3,\ m_3 = 1$
(C):	-1	0	0	$m_1 = 3,\ m_2 = \lambda\sqrt{\frac{3}{2}} + 3,\ m_3 = 1$
(D):	$\frac{\lambda}{\sqrt{6}}$	$(1 - \frac{\lambda^2}{6})^{\frac{1}{2}}$	0	$m_1 = \lambda^2 - 3,\ m_2 = \frac{\lambda^2}{2} - 3,\ m_3 = \frac{\lambda^2}{2} - 2$
(E):	$\frac{1}{\lambda}\sqrt{\frac{3}{2}}$	$\frac{1}{\lambda}\sqrt{\frac{3}{2}}$	0	$m_1 = -\frac{1}{2},\ m_2 = -\frac{3}{4}\left[1 - \sqrt{\frac{24}{\lambda^2} - 7}\right],\ m_3 = -\frac{3}{4}\left[1 + \sqrt{\frac{24}{\lambda^2} - 7}\right]$
(F):	0	0	1	$m_1 = -1,\ m_2 = 2,\ m_3 = 1$
(G)	$\frac{2}{\lambda}\sqrt{\frac{2}{3}}$	$\frac{1}{\lambda}\sqrt{\frac{4}{3}}$	$\sqrt{1 - \frac{4}{\lambda^2}}$	$m_1 = 1,\ m_2 = -\frac{1}{2} - \frac{1}{2\lambda}\sqrt{64 - 15\lambda^2},\ m_3 = -\frac{1}{2} + \frac{1}{2\lambda}\sqrt{64 - 15\lambda^2}$

We notice that the first five points, (A) to (E), are the same as the 2D system if we take $\gamma = 1$ and so have the same stability. From analysis of the eigenvalues, we see that point (F) is half stable and (G) is unstable for $64/15 > \lambda^2$ and a spiral saddle point for $64/15 < \lambda^2$.

3.4 Numerical Solutions (3D)

To solve numerically we extend the method described in section 2.4 by making $d\boldsymbol{x}/dt$ a three-component vector containing equations (73), (74) and (75). We must also specify three initial conditions. Like before, the code was run multiple times to plot a range of trajectories. The numerical solutions are shown in figures 7 to 11. The boundary between accelerating and non-accelerating regions has been included by plotting the acceleration condition using the Meshgrid function in MATLAB.

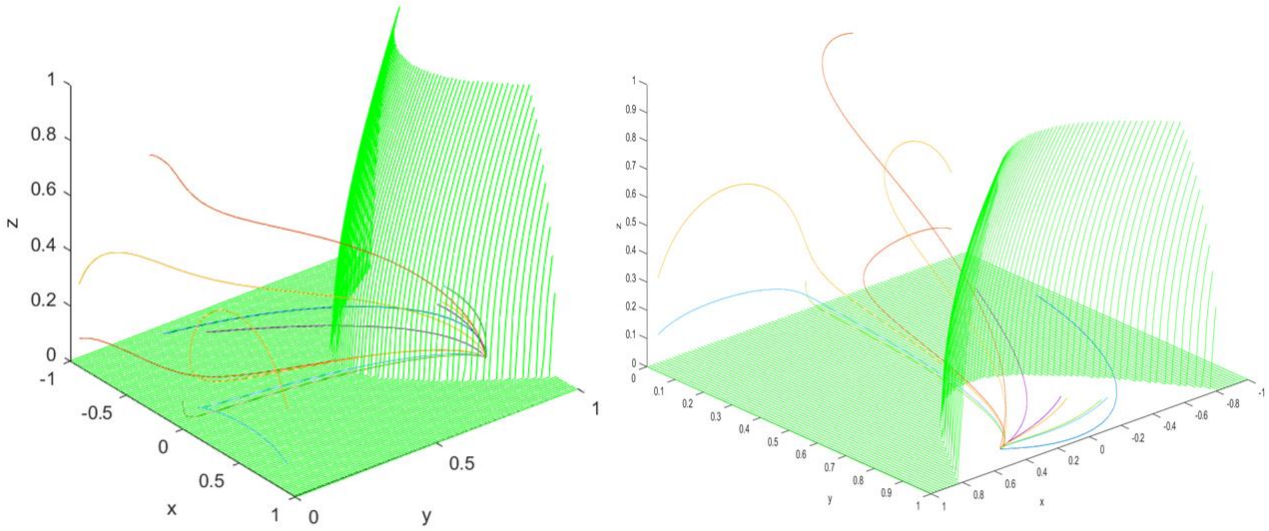

Figure 7: Phase plane of 3D system for $\lambda = 1$. Front and back views pictured from left to right. Boundary between accelerating and non-accelerating regions shown in green. Trajectories converge at fixed point $x = 1/\sqrt{6}, y = \sqrt{5/6}, z = 0$ corresponding to point (D). Point lies inside accelerating region and so is a dark energy solution.

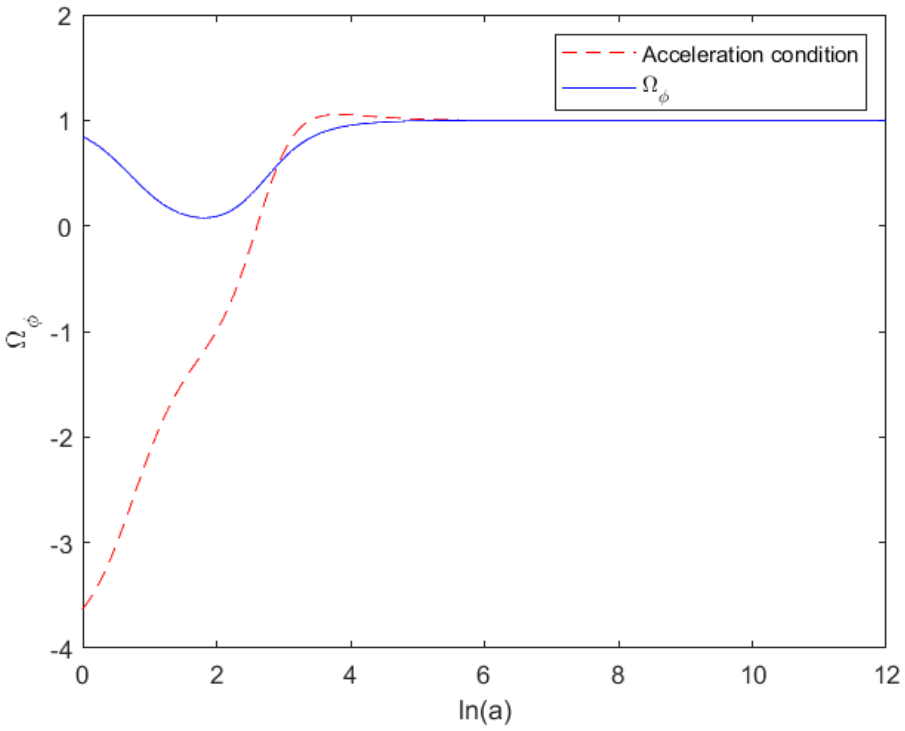

Figure 8: Plot of Ω_ϕ against $\ln(a)$ for $\lambda = 1$ shown in blue. Plotted with initial conditions $x = -0.92$, $y = 0.001$ and $z = 0.3$. Acceleration condition denoted by red-dashed line. System first crosses into accelerating regime at $\ln(a) = 1.26$ when $\Omega_\phi = 0.567$. Scalar field dominates in late times.

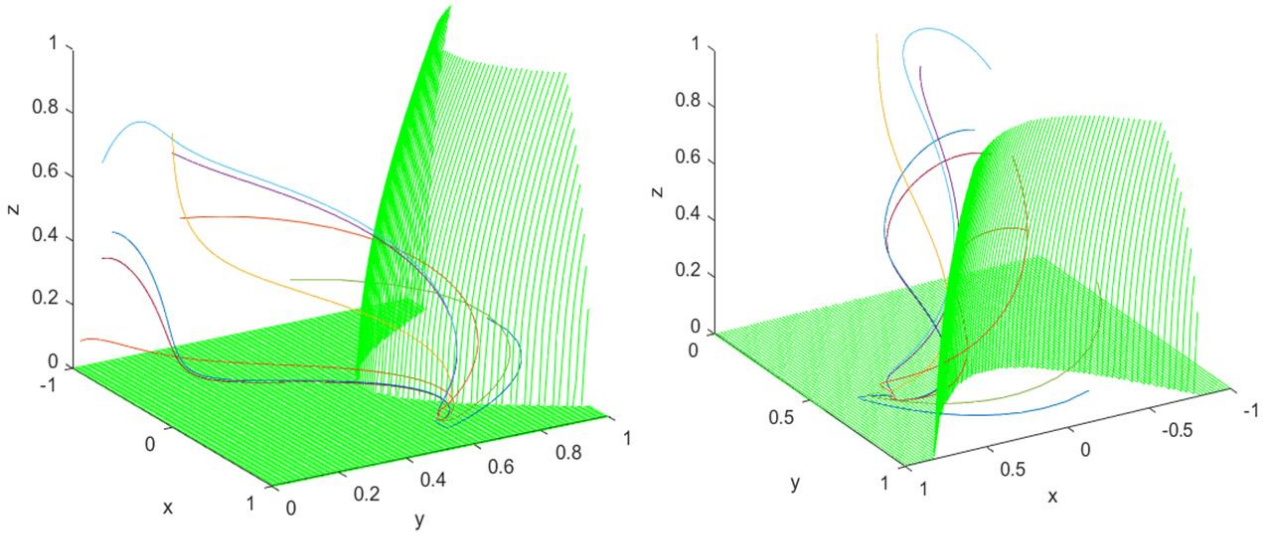

Figure 9: Phase plane of 3D system for $\lambda = 2$. Front and back views pictured from left to right. Boundary between accelerating and non-accelerating regions shown in green. Trajectories converge at fixed point $x = y = \sqrt{6}/4$, $z = 0$ corresponding to point (E). Point lies outside accelerating region.

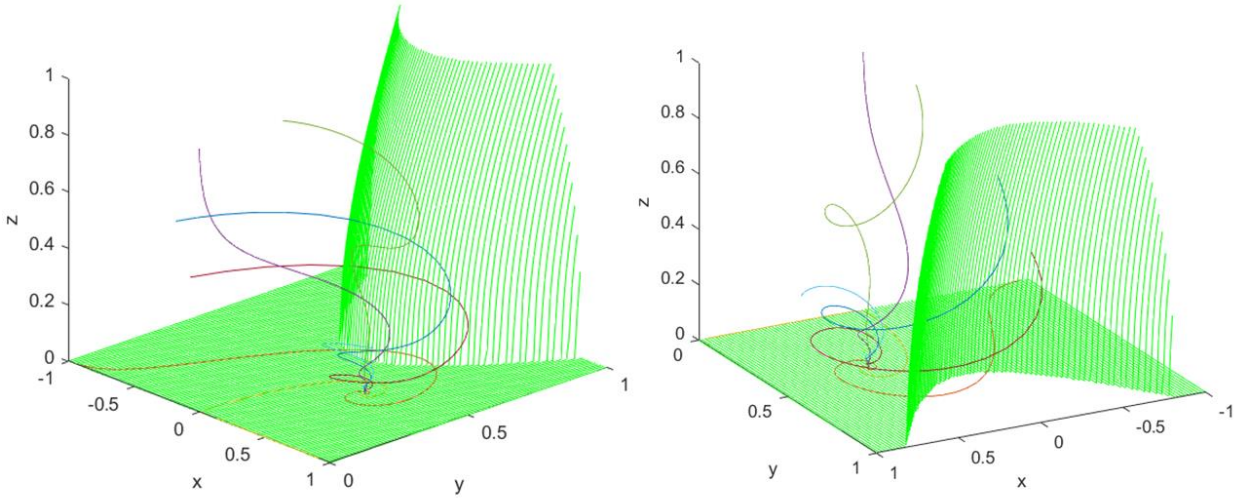

Figure 10: Phase plane of 3D system for $\lambda = 3$. Front and back views pictured from left to right. Boundary between accelerating and non-accelerating regions shown in green. Trajectories converge at fixed point $x = y = \sqrt{6}/6, z = 0$ corresponding to point (E) and from trajectories we see the point is a stable spiral. Point lies outside accelerating region.

3.5 Results and Discussion (3D)

For our new model universe, we can summarize all the fixed points and their properties in table 5 below.

Table 5: Fixed points of 3D system with associated properties

Point:	x	y	z	Existence criteria:	Stability:	Ω_ϕ	γ_ϕ	Acceleration:
(A)	0	0	0	$All\ \lambda$	$Saddle\ point\ for\ all\ \lambda$	0	$undefined$	No
(B)	1	0	0	$All\ \lambda$	$Unstable\ node\ for\ \lambda < \sqrt{6}$ $Saddle\ point\ for\ \lambda > \sqrt{6}$	1	2	No
(C)	-1	0	0	$All\ \lambda$	$Unstable\ for\ \lambda > \sqrt{6}$ $Saddle\ point\ for\ \lambda < -\sqrt{6}$	1	2	No
(D)	$\frac{\lambda}{\sqrt{6}}$	$(1-\frac{\lambda^2}{6})^{\frac{1}{2}}$	0	$\lambda^2 < 6$	$Stable\ for\ \lambda^2 < 3$ $Saddle\ point\ for\ 3 < \lambda^2 < 6$	1	$\frac{\lambda^2}{3}$	$For\ \lambda^2 < 2$
(E)	$\frac{1}{\lambda}\sqrt{\frac{3}{2}}$	$\frac{1}{\lambda}\sqrt{\frac{3}{2}}$	0	$\lambda^2 > 3$	$Stable\ for\ 3 < \lambda^2 < \frac{24}{7}$ $Stable\ spiral\ for \lambda^2 > \frac{24}{7}$	$\frac{3}{\lambda^2}$	1	No
(F)	0	0	1	$All\ \lambda$	$Saddle\ point\ for\ all\ \lambda$	0	$undefined$	No
(G)	$\frac{2}{\lambda}\sqrt{\frac{2}{3}}$	$\frac{1}{\lambda}\sqrt{\frac{4}{3}}$	$\sqrt{1-\frac{4}{\lambda^2}}$	$\lambda^2 > 4$	$Spiral\ saddle\ point\ for\ \lambda^2 > \frac{64}{15}$ $Unstable for\ 4 < \lambda^2 < \frac{64}{15}$	$\frac{4}{\lambda^2}$	$\frac{4}{3}$	No

For the fixed points (A) to (E) we make the same conclusions as presented in section 2.5 with (D) being the stable dark energy solution and (E) being a tracking solution. We now see however, that (E) tracks the contribution from matter as it has the corresponding equation of state and again conclude that this is more stable than the dark energy solution due to the crossover of stability regimes.

From the last two points, (F) makes no contribution to the density parameter at late times so can be discarded. Point (G) is of interest as it has an effective equation of state $\gamma_\phi = 4/3$. This matches the contribution from radiation and so we identify it as another tracking solution. We notice however, that (E) will still be the preferential fixed point since, in the range for which (G) is a saddle point, (E) is always stable. The numerical plots support this as can be seen in figure 11 wherein λ is chosen specifically to lie within the range for which (G) is a saddle point.

Although we have made valuable insight into the behavior of the field in late times, we must still conclude that such a scalar field is likely not a dark energy candidate. It's clear then, that modification of the scalar field itself is necessary to continue the investigation.

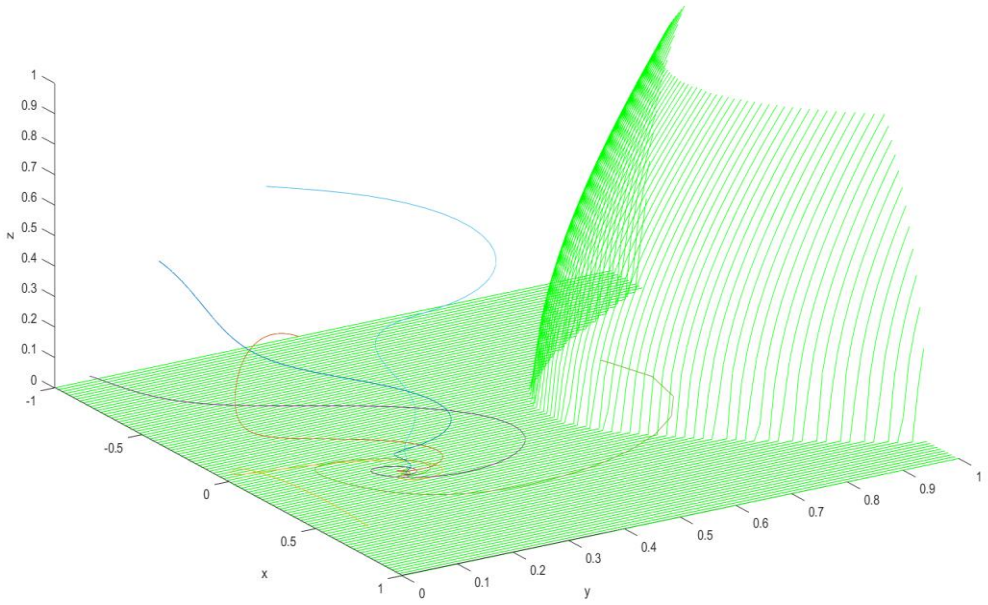

Figure 11: Phase plane of 3D system for $\lambda = 5$. Boundary between accelerating and non-accelerating regions shown in green. Trajectories converge at fixed point $x = y = 0.244$, $z = 0$ corresponding to point (E). Value of λ chosen to lie within range for which (G) is half stable. Despite this choice, system converges at point (E) proving it to be a more stable solution.

4. Modified Potential

We consider a modification to the scalar field such that the potential includes two exponentials. By inspection, we see that a product will result in a system with identical properties as described in section 3 and so conclude that our new potential must take the form,

$$V = Ae^{-k\lambda\phi} + Be^{-k\sigma\phi}, \tag{79}$$

where we introduce a new parameter, σ, corresponding to the growth rate of the second exponential. If we then express (79) as $V = V_1 + V_2$ with $V_1 = Ae^{-k\lambda\phi}$ and $V_2 = Be^{-k\sigma\phi}$, the new evolution equations are trivial to find as they remain in the form of (36), (37), (67), (68), (69) and (70) with the exception that $V = V_1 + V_2$ and $dV/dt = dV_1/dt + dV_2/dt$.

To write as an autonomous system, we again postulate that the Friedmann equation can be written as,

$$\frac{\rho_m k^2}{3H^2} = 1 - x^2 - {y_1}^2 - {y_2}^2 - z^2 \tag{80}$$

and so derive the new variables,

$$y_1 = \frac{k\sqrt{V_1}}{\sqrt{3}H}, \quad y_2 = \frac{k\sqrt{V_2}}{\sqrt{3}H} \tag{81}$$

with x and z still given by (40) and (72).

The 4D autonomous system is then,

$$x' = -3x + \lambda\sqrt{\frac{3}{2}}{y_1}^2 + \sigma\sqrt{\frac{3}{2}}{y_2}^2 + x\left[2z^2 + 3x^2 + \frac{3}{2}(1 - x^2 - {y_1}^2 - {y_2}^2 - z^2)\right], \quad (82)$$

$${y_1}' = -\lambda\sqrt{\frac{3}{2}}xy_1 + y_1\left[3x^2 + 2z^2 + \frac{3}{2}(1 - x^2 - {y_1}^2 - {y_2}^2 - z^2)\right], \quad (83)$$

$${y_2}' = -\sigma\sqrt{\frac{3}{2}}xy_2 + y_2\left[3x^2 + 2z^2 + \frac{3}{2}(1 - x^2 - {y_1}^2 - {y_2}^2 - z^2)\right], \quad (84)$$

$$z' = -2z + 2z^3 + z\left[3x^2 + \frac{3}{2}(1 - x^2 - {y_1}^2 - {y_2}^2 - z^2)\right]. \quad (85)$$

The density parameter (55) and effective equation of state (58) are easily modified for the new system and are given by,

$$\Omega_\phi = x^2 + {y_1}^2 + {y_2}^2 \quad (86)$$

and

$$\gamma_\phi = \frac{2x^2}{x^2 + {y_1}^2 + {y_2}^2}. \quad (87)$$

The acceleration condition, (76), can be modified in the same way and is hence,

$$3{y_1}^2 - 3{y_2}^2 - 3x^2 - z^2 > 1. \quad (88)$$

To find the fixed points, we first notice that when $y_2 = 0$ the system reduces to the 3D system specified by equations (73), (74) and (75) and so has the same fixed points and stability. The same applies for when $y_1 = 0$ except with the replacement of λ with σ. This gives the first ten fixed points, labeled (A) to (J) in tables 6 and 7. For the last fixed point, we take a different approach and recall that a suitable dark energy candidate would have an equation of state given by $w = (\gamma - 1) = -1$. Throughout the investigation ϕ has been spatially constant however, if ϕ is also temporally constant then we find $\frac{p_\phi}{\rho_\phi} = w = -1$ as required. Taking this to be the case, we find that $x = 0$ and so when $y_1 \neq 0$ and $y_2 \neq 0$ we derive the final fixed point,

$$x = 0,\ y_1 = \sqrt{\frac{\sigma}{\sigma - \lambda}},\ y_2 = \sqrt{\frac{\lambda}{\lambda - \sigma}},\ z = 0, \quad (89)$$

labeled (K) in table 7.

The stability analysis is easily extended in the same way as the extension from 2D. For conciseness, we shall simply state the new stability conditions on the fixed points in tables 6 and 7 in section 4.1.

4.1 Results and Discussion (4D)

Finally, we summarize all the fixed points, labeled (A) to (K) and their properties in tables 6 and 7 below.

Table 6: Fixed points A to F and associated properties

Point:	x	y_1	y_2	z	Existence criteria:	Stability:	Ω_ϕ	γ_ϕ	Acceleration condition satisfied?
(A)	0	0	0	0	$All\ \lambda\ and\ \sigma$	$Saddle\ point\ for\ all\ \lambda\ and\ \sigma$	0	$undefined$	No
(B)	1	0	0	0	$All\ \lambda\ and\ \sigma$	$Unstable\ node\ for\ \lambda < \sqrt{6},\ \sigma < \sqrt{6}$ $Else\ a\ saddle\ point$	1	2	No
(C)	-1	0	0	0	$All\ \lambda\ and\ \sigma$	$Unstable\ for\ \lambda > \sqrt{6},\ \sigma > \sqrt{6}$ $Else\ a\ saddle\ point$	1	2	No
(D)	$\frac{\lambda}{\sqrt{6}}$	$(1-\frac{\lambda^2}{6})^{\frac{1}{2}}$	0	0	$\lambda^2 < 6$	$Stable\ for\ \lambda^2 < 3,\ \lambda < \sigma, (\lambda > 0)$ $Saddle\ point\ for\ 3 < \lambda^2 < 6$	1	$\frac{\lambda^2}{3}$	$For\ \lambda^2 < 2$
(E)	$\frac{1}{\lambda}\sqrt{\frac{3}{2}}$	$\frac{1}{\lambda}\sqrt{\frac{3}{2}}$	0	0	$\lambda^2 > 3$	$Stable\ for\ 3 < \lambda^2 < \frac{24}{7},\ \lambda < \sigma, (\lambda > 0)$ $Stable\ spiral\ for\ \lambda^2 < \frac{24}{7}$ $Half\ stable\ spiral\ for\ \lambda > \sigma$	$\frac{3}{\lambda^2}$	1	No
(F)	0	0	0	1	$All\ \lambda\ and\ \sigma$	$Saddle\ point\ for\ all\ \lambda\ and\ \sigma$	0	$undefined$	No

Table 7: Fixed points G to K and associated properties

Point:	x	y_1	y_2	z	Existence criteria:	Stability:	Ω_ϕ	γ_ϕ	Acceleration condition satisfied?
(G)	$\frac{2}{\lambda}\sqrt{\frac{2}{3}}$	$\frac{1}{\lambda}\sqrt{\frac{4}{3}}$	0	$\sqrt{1-\frac{4}{\lambda^2}}$	$\lambda^2 > 4$	$Unstable\ for\ 4 < \lambda^2 < \frac{64}{15},\ \lambda > \sigma, (\lambda > 0)$ $Spiral\ saddle\ point\ for\ \lambda^2 > \frac{64}{15}$	$\frac{4}{\lambda^2}$	$\frac{4}{3}$	no
(H)	$\frac{\sigma}{\sqrt{6}}$	0	$\sqrt{1-\frac{\sigma^2}{6}}$	0	$\sigma^2 < 6$	$Stable\ for\ \sigma^2 < 3,\ \sigma < \lambda, (\sigma > 0)$ $Half\ stable\ for\ 3 < \sigma^2 < 6,$	1	$\frac{\sigma^2}{3}$	$\sigma^2 < 2$
(I)	$\frac{1}{\sigma}\sqrt{\frac{3}{2}}$	0	$\frac{1}{\sigma}\sqrt{\frac{3}{2}}$	0	$\sigma^2 > 3$	$Stable\ for\ 3 < \sigma^2 < \frac{24}{7},\ \lambda > \sigma, (\sigma > 0)$ $Stable\ spiral\ for\ \sigma^2 > \frac{24}{7}$	$\frac{3}{\sigma^2}$	1	no
(J)	$\frac{2}{\sigma}\sqrt{\frac{2}{3}}$	0	$\frac{1}{\sigma}\sqrt{\frac{4}{3}}$	$\sqrt{1-\frac{4}{\sigma^2}}$	$\sigma^2 > 4$	$Unstable\ for\ 4 < \sigma^2 < \frac{64}{15},\ \sigma > \lambda, (\sigma > 0)$ $Spiral\ saddle\ point\ for\ \sigma^2 > \frac{64}{15}$	$\frac{4}{\sigma^2}$	$\frac{4}{3}$	no
(K)	0	$\sqrt{\frac{\sigma}{\sigma-\lambda}}$	$\sqrt{\frac{\lambda}{\lambda-\sigma}}$	0	$\lambda\ and\ \sigma$ $have\ opposite\ signs$	$Stable\ spiral\ for\ \frac{3}{4} < \lvert\lambda\sigma\rvert$ $Stable\ for \frac{3}{4} > \lvert\lambda\sigma\rvert$	1	0	$For\ all\ \lambda\ and\ \sigma$

From the stability conditions we see there are two regimes to consider. First, we shall consider the case when λ and σ have the same sign. In this regime, the points of interest are (D), (E), (G), (H), (I) and (J). Points (D) and (H) are dark energy solutions and the rest are tracking solutions mimicking the contribution from matter and radiation. Although (D) and (H) are both stable, closer analysis of the stability shows that the matter tracking solutions (I) and (E) are still the preferential fixed points.

Let us now consider the more interesting second case when λ and σ have opposite signs. There is now an extra dark energy solution, (K), that accelerates for all values of λ and σ. Furthermore, unlike our previous accelerating solutions, we find it to be always stable. Finally, let us compare this point with the other stable points, (D), (E), (H) and (I). We clearly see that the existence criteria on (K) contradicts the conditions required for the aforementioned points to be stable. Therefore, in this regime, we conclude that our dark energy solution, (K), will be the preferential fixed point of the system.

Both regimes should be treated as equally likely since there is no reason to suggest one is more plausible than the other from this investigation alone. Despite this, the existence of a such a strong dark energy solution, along with the existence of possible stable ones in the other regime, is certainly evidence in support of a scalar field with a potential, (79), as a candidate for the source of dark energy observed in the universe today.

Another noteworthy result can be found by solving the modified system numerically, once again, by extending the method used in previous sections. It can be demonstrated that, for specific choices of λ, there can exist temporary periods of acceleration when the density parameter reaches the values exhibited by dark energy today. This is demonstrated in figure 12 and, if we except a scalar field as a viable dark energy candidate, may suggest today's acceleration is only temporary. We also notice that, when this is the case, the field dominates at late times but the solution does not accelerate. This behavior, exhibited by points (B) and (C) in all sections, only occurs when $x^2 = 1$. Since x goes as $\dot{\phi}$, we interpret this as domination by the effective kinetic energy of the field. This leads us to conclude that these eras of possible temporary expansion occur when the effective kinetic energy of the field dominates. The result also implies that only the contribution from the potential causes acceleration as we notice for all the accelerating solutions, $y \neq 0$.

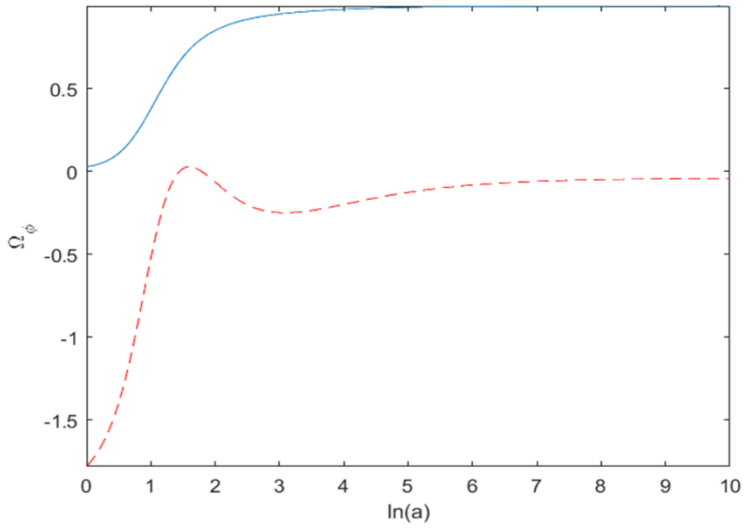

Figure 12: Plot of Ω_ϕ against $\ln(a)$ for $\lambda = 1.428$ and $\sigma = 2$ in blue. Acceleration condition denoted by red dashed line. From acceleration condition there is a temporary period of accelerating expansion when $\Omega_\phi = 0.6719$ which is consistent with current observations of dark energy.

5. Conclusion

In summary, we considered a flat FRW model universe containing a general fluid and showed that a scalar field with an exponential potential leads to a dark energy solution and a tracking solution, in which the field mimics the contribution from the fluid. We evaluate this as insufficient evidence for dark energy as we have argued that the tracking solution is the preferential fixed point of the system. The same conclusion is made when the model is expanded to contain matter and radiation simultaneously. We find two tracking solutions, one mimicking matter and one, radiation as well as the initial dark energy solution. In this case, the matter tracking solution is the preferential fixed point. Finally, we made a modification to the scalar field by changing the potential to a sum of exponentials. This gave two regimes. In the first, the previous solutions exist along with counter parts in terms of the new parameter σ. In the second, we identified one stable dark energy solution which is the preferential fixed point and so conclude that a scalar field with a potential of (79) is a viable dark energy candidate. It was also noted that temporary periods of acceleration can exist when the kinetic contribution of the field dominates which could align with the acceleration we experience today.

This investigation does not provide conclusive identification of the source of dark energy but does show scalar fields should not be discarded. Aside from dark energy, an investigation of this nature provides valuable insight into the behavior of such fields allowing observational cosmologists, as well as particle physicists, to better target future research. Future studies could further constrain the values of λ and σ to determine which regimes are more physical as well as explore the possibilities of temporary accelerating eras.

References:

[1] Hubble, E., A relation between distance and radial velocity among extra-galactic nebulae, National Academy of Sciences, 15,3, 168-173, (1929)

[2] Adam, G. Riess, et al. Observational Evidence from Supernovae for an Accelerating Universe and a Cosmological Constant, American Astronomical Society, 116, 3, 1009-1038, (1998)

[3] M.P Hobson, G.Efstathiou and A.N Lasenby. General Relativity, An introduction for physicists. Cambridge university press, (2006)

[4] Copeland, Edmund J.; Sami, M.; Tsujikawa, Shinji, Dynamics of dark energy, INTERNATIONAL JOURNAL OF MODERN PHYSICS D, 15, 11, 1753-1935, (2006)

[5] Aghanim, N, et al. Planck 2018 results: VI. Cosmological parameters, ASTRONOMY AND ASTROPHYSICS, 641, (2020)

[6] Vikman, A. Can dark energy evolve to the phantom?, Physical Review D, 71, 2, 023515, (2005)

[7] Nussbaumer, H. Slipher's Redshifts as Support for de Sitter's Model and the Discovery of the Dynamic Universe, ORIGINS OF THE EXPANDING UNIVERSE: 1912-1932, Astronomical Society of the Pacific Conference Series, 471, 25-38, (2013)

[8] S.E. Rugh, H. Zinkernagel, The quantum vacuum and the cosmological constant problem, Studies in History and Philosophy of Science Part B: Studies in History and Philosophy of Modern Physics, 33, 4, 663-705, (2002)

[9] Cao, Tian and Schweber, Silvan, The conceptual foundations and the philosophical aspects of renormalization theory, Synthese, 97, 33-108, (1993)

[10] Srednicki, M. Quantum Field Theory, Cambridge University Press, (2007)

[11] S. Chatrchyan, et al. Observation of a new boson at a mass of 125 GeV with the CMS experiment at the LHC, Physics Letters B, 716, 1, 30-61, (2012)

[12] Copeland, E., Liddle, A. and Wands, D., Exponential potentials and cosmological scaling solutions. Physical Review D, 57,8 ,4686-4690, (1998)